

A Clinicopathological Study of Young-onset Hepatocellular Carcinoma

KWAN-YUNG AU¹, KRISTY KWAN-SHUEN CHAN¹ and REGINA CHEUK-LAM LO^{1,2}

¹Department of Pathology, The University of Hong Kong, Hong Kong, P.R. China;

²State Key Laboratory of Liver Research, The University of Hong Kong, Hong Kong, P.R. China

Abstract. *Background/Aim:* The aim of this study was to describe the clinicopathological features of hepatocellular carcinoma (HCC) diagnosed at 40 years of age or below. *Materials and Methods:* Expression of CK19, Glypican-3 and β -catenin was assessed in clinical samples by immunohistochemistry (IHC). IHC expression was correlated with clinicopathological parameters. Hotspot mutations in TP53 gene were analyzed by sequencing. *Results:* Thirty-six cases were included with a male to female ratio of 3:1. Eighty percent of cases were associated with chronic hepatitis B infection. CK19 and GPC3 were expressed in 61% and 56% of cases, respectively. Only one case demonstrated β -catenin over-expression. TP53 hotspot mutation was identified in 4 cases. Number of tumor nodules, vascular invasion, and preoperative serum AFP level were associated with prognosis. *Conclusion:* A higher CK19 expression rate was observed in our young-onset HCC cohort, whereas β -catenin pathway activation and TP53 gene mutation events were less frequent. Conventional clinicopathological parameters remain predictors of survival.

Hepatocellular carcinoma (HCC) is a major cancer worldwide, showing a male predominance. Local data revealed a mean age of diagnosis at 65 years for men and 73 years for women (Hong Kong Cancer Registry, Hospital Authority, 2015). Occurrence of HCC in the younger age group is relatively rare. Pediatric and adolescent HCC (below 20 years of age) has been reported to constitute less than 1% of HCC (1). For chronic hepatitis B patients, young-onset HCC was defined as a diagnosis under 40 years of age

for men and 50 years of age for women according to the American Association for the Study of Liver Diseases (AASLD) guidelines. In particular, clinicopathological features of HCC in the younger age group exhibit some differences compared to the older age group. Early-onset HCC (under 40 years of age) is largely related to ethnic factors (2) and encompasses a broader spectrum of etiological factors such as hepatitis B virus (HBV), hepatitis C virus, tyrosinemia, biliary atresia, Alagille syndrome, glycogen storage disease, *etc.* (3, 4). On histological examination, the fibrolamellar HCC subtype comprised 15-41% cases in a meta-analysis (4). In terms of prognosis, compared to adult HCC patients, pediatric patients present with longer overall survival (7.98 vs. 2.78 years) (5). While genomic changes in HCC including *TERT*, *TP53*, *CTNNB1*, *TSC*, *ARID1A* mutations have been reported in many studies (6), little is known about the subset of young-onset HCC. A recent study has reported on the genetic alterations in a cohort of 15 pediatric HCC patients, among which 6 were associated with non-hepatotropic virus diseases, while the remaining 9 had no underlying liver disease (7). Among these 15 patients, 4 were found to have *CTNNB1* deletion. A *TP53*, *TERT* and *APC* mutation was identified in 1, 2, and 2 patients, respectively (7). This prompted us to examine the clinicopathological characteristics of our local young-onset HCC. Specifically, we focused on the expression of cytokeratin 19 (CK19), Glypican-3 (GPC3), and β -catenin. In addition, we analyzed the mutation status of *TP53*, the most commonly mutated tumor suppressor gene in HCC (8).

CK19 is an intermediate filament in the cytoplasm of epithelial cells. In the context of primary liver cancer, CK19 had been known as a biliary marker. It was only recently found to be expressed in some HCCs, signifying an intermediate phenotype between hepatocellular and biliary differentiation of tumor cells. The expression rate of CK19 in HCC samples ranged from 10-35.7% (9-12). Compared to CK19- HCC, CK19+ HCC demonstrated a lower overall survival rate (80.4% vs. 28.9% at 5 years) and disease-free

Correspondence to: Regina Cheuk-Lam Lo, Department of Pathology, The University of Hong Kong, Queen Mary Hospital, Pokfulam, Hong Kong SAR, P. R. China. Tel: +852 22552688, e-mail: reginalo@pathology.hku.hk

Key Words: Liver cancer, young-onset, mutation, immunohistochemistry.

Table I. PCR Primers and annealing temperature.

| Gene (region of exon) | Primer | Annealing temperature (°C) |
|----------------------------|----------------------------|----------------------------|
| TP53 exon 5 (upper region) | 5'-CCTCTTCCTACAGTACTCCC-3' | 59 |
| | 5'-AACCTCCGTCATGTGCTGTG-3' | |
| TP53 exon 5 (lower region) | 5'-GTGCAGCTGTGGGTTGATTC-3' | 57 |
| | 5'-GCTGCTCACCATCGCTATCT-3' | |
| TP53 exon 7 (whole exon) | 5'-AGGTTGGCTCTGACTGTACC-3' | 57 |
| | 5'-CTCCTGACCTGGAGTCTTCC-3' | |

survival rate (54.5% vs. 34.3% at 3 years) after surgical resection (12). GPC3 is a membrane-bound proteoglycan, in a meta-analysis from our group (13). Expression is absent in the normal liver and benign liver diseases, rendering it a key marker for distinguishing HCC from its precursor lesion (14). Similar to CK19, high GPC3 expression in HCC tissues was found to confer poor prognostic outcome (15).

TP53 and *CTNNB1* mutations have been identified in 30-37.2% (8, 16-19) and 12.8-35.7% of clinical samples (8, 16, 20), respectively. Notably, Wnt/ β -catenin pathway and *TP53* alterations in HCC have been shown to be mutually exclusive molecular events (16, 21). In a study on profiling *TP53* mutation status by Woo *et al.* (18) in a Chinese HCC cohort (n=329), 125 cases harbored a *TP53* mutation. Among these 125 cases, R249S (61.6%, 77 cases) and V157F (6.4%, 8 cases) were the two most common *TP53* mutations. R249S in codon 249 in exon 7 is characterized by the G:C to T:A transversion at the third base of the *TP53* codon 249, which leads to an amino acid substitution from arginine to serine. In terms of prevalence, R249S demonstrates a geographic variation with a high prevalence (40-77%) in high-aflatoxin exposure regions, such as China and Africa, whereas it is less frequent in the white population. V157F is a missense mutation characterized by the G:C to T:A transversion at the first base of the *TP53* codon 157, leading to an amino acid change from valine to phenylalanine. Hotspot mutations of *TP53* at codons 249 and 157 have been correlated with poorer prognosis (18, 22). R249S and V157F confer a significantly shorter overall survival rate with a hazard ratio of 1.98 and 4.25, respectively, compared to wild-type *TP53* HCC patients (18). *CTNNB1* mutations have been found in 20-40% of all HCC cases worldwide (23-25). The lowest overall *CTNNB1* mutation rate of 15.9% was observed in Asians (24). Most *CTNNB1* mutations occur in exon 3, a region encoding for the protein sequence containing consensus sites for phosphorylation (24). *CTNNB1* mutations lead to the stabilization and nuclear translocation of the protein, with the latter readily detectable by immunohistochemical staining. β -catenin accumulation in the cytoplasm and/or the nucleus has been reported in 10-50% of HCC cases (11, 26-28).

In this study, we studied the clinicopathological features of a cohort of young-onset HCC (below 40 years of age) in our center. Pathologically, immunohistochemical (IHC) expression of CK19, GPC3, and β -catenin together with the mutation status of *TP53* were examined.

Materials and Methods

Clinical samples. Surgical resection specimens of HCC were retrospectively identified and retrieved from the pathology archive of Queen Mary Hospital, a tertiary referral center in Hong Kong. Cases with surgical resection performed when the patient was 40 years or younger were chosen. Patients with recurrence or those who received neoadjuvant therapy were excluded. The histology sections were reviewed by a pathologist (R.C.L.) to confirm the diagnosis. Fibrolamellar HCC was excluded. A representative tumor block was selected from each case for subsequent analyses. Clinical data were retrieved from medical records. Use of human clinical samples was approved by the institutional review board of the University of Hong Kong/Hospital Authority Hong Kong West Cluster.

DNA extraction. Ten 10- μ m thick tissue sections were cut from formalin-fixed paraffin-embedded (FFPE) tissue blocks for DNA extraction. The sections were dewaxed and rehydrated in xylene and decreasing concentrations of ethanol. Hematoxylin and eosin-stained slides of each FFPE tissue block were evaluated by a pathologist (R.C.L.) and the region of interest was marked. DNA was extracted from the region of interest using QIAamp DNA FFPE Tissue Kit (Qiagen, Hilden, Germany) according to the manufacturer's protocol. DNA quantification was performed by BioDrop- μ LITE (BioDrop, Cambridge, UK). Extracted DNA was stored at -20°C prior to use.

Polymerase chain reaction (PCR) and Sanger sequencing. PCR reaction was performed in a 15 μ l reaction volume containing 100-200 ng of genomic DNA, 1 μ M of each primer, 0.2 mM of dNTP Mix, 1 U of AmpliTaq Gold™ DNA Polymerase with 1x PCR Buffer II and 1.5 mM of MgCl₂ (Applied Biosystems, Foster City, CA, USA). A touchdown PCR program was adopted and the conditions were as follows: For *TP53* exon 7, initial denaturation performed at 94°C (9 min) for 1 cycle, followed by 5 cycles of 94°C (1 min), 62°C (1.5 min) and 72°C (2 min), where the annealing temperature was decreasing 1°C/cycle, followed by 35 cycles at 94°C (1 min), 57°C (1.5 min) and 72°C (2 min). Final extension was performed at 72°C for 7 min. For *TP53* exon 5, the annealing temperature was set at either 62°C or 64°C initially, decreasing

Table II. Clinicopathological parameters of the hepatocellular carcinoma (HCC) patients in our cohort.

| Case | Gender/age | Single(s)/multiple (m) nodules | Size of largest nodule (cm) | Vascular invasion | Primary liver disease | Pre-operative AFP (IU/ml) |
|--------|------------|--------------------------------|-----------------------------|-------------------|-----------------------|---------------------------|
| HCC-1 | M/22 | M | 10 | + | HBV | 19,530 |
| HCC-2 | M/29 | S | 3.8 | – | HBV | 2 |
| HCC-3 | M/27 | M | 7 | + | – | 7,860 |
| HCC-4 | M/25 | M | 13 | + | HBV | 162,763 |
| HCC-5 | F/18 | M | 14 | – | – | 705.5 |
| HCC-6 | M/26 | M | N/A | + | HBV | 174,051 |
| HCC-7 | M/20 | S | 1.5 | – | HBV | 419,980 |
| HCC-8 | M/12 | S | 1.5 | – | HBV | 158.53 |
| HCC-9 | F/25 | S | 2.8 | – | HBV | 1,305.6 |
| HCC-10 | M/27 | M | 19.5 | + | – | 4,440.5 |
| HCC-11 | M/28 | S | 1.5 | + | HBV | 2,362.2 |
| HCC-12 | M/28 | S | 2.2 | + | HBV | 17.43 |
| HCC-13 | M/24 | M | 12 | + | – | 13,887 |
| HCC-14 | F/24 | S | 9.5 | + | – | 37,119 |
| HCC-15 | F/9 | S | 5 | – | HBV | 659.02 |
| HCC-16 | M/39 | S | 8 | + | HBV | 9.13 |
| HCC-17 | F/36 | S | 12 | – | HCV | 23,016 |
| HCC-18 | F/31 | S | 9 | + | HBV | 630.8 |
| HCC-19 | M/34 | S | 2 | + | HBV | 16.6 |
| HCC-20 | M/34 | S | 23 | + | HBV | N/A |
| HCC-21 | M/39 | S | 5.5 | – | HBV | 4.98 |
| HCC-22 | M/40 | S | 18.5 | + | HBV | 109,726 |
| HCC-23 | M/35 | M | 4.5 | + | HBV | 3320 |
| HCC-24 | M/36 | S | 3.5 | – | HBV | 145.25 |
| HCC-25 | M/40 | M | 2.8 | – | HBV | 4.15 |
| HCC-26 | F/38 | M | 3.5 | + | HBV | 1,648.4 |
| HCC-27 | M/40 | M | 8 | + | HBV | 4.98 |
| HCC-28 | M/32 | S | 3.5 | + | HBV | 2.49 |
| HCC-29 | F/31 | S | 1.5 | – | HBV | 24.07 |
| HCC-30 | M/38 | M | 17 | + | HBV | 524,063 |
| HCC-31 | F/39 | M | 9 | + | HBV | 35,376 |
| HCC-32 | M/40 | S | 2.5 | + | HCV | 5.81 |
| HCC-33 | M/32 | S | 10 | + | HBV | 3.32 |
| HCC-34 | M/39 | S | 11 | + | HBV | 155,262 |
| HCC-35 | M/39 | S | 1.5 | – | HBV | 101.26 |
| HCC-36 | M/39 | S | 4.5 | – | HBV | 3.32 |

M: Male; F: female; HBV: hepatitis B virus.

1°C/cycle in the first 5 cycles. PCR products were separated using electrophoresis and visualized in a 1.5-2% agarose gel with SYBR®Safe DNA Gel Stain (Invitrogen, Hercules, CA, USA) using Molecular Imager® Gel Doc™ XR+ System with Image Lab™ Software (Bio-Rad, Hercules, CA, USA). DNA fragment was purified from agarose gel using GeneJET Gel Extraction Kit (ThermoFisher Scientific, Waltham, MA, USA). Either purified DNA fragment or PCR products were subjected to Sanger sequencing using 3730xl DNA Analyzer or 3500xl Genetic Analyzer (Applied Biosystems). PCR Primers are listed in Table I.

Immunohistochemical staining and analysis. Four-µm FFPE tissue sections were used. After dewaxing and rehydration, tissue sections were subjected to heat-induced epitope retrieval using Tris-EDTA (pH9.0). 3% hydrogen peroxide and serum-free protein block

(Dako, Carpinteria, CA, USA) were used as blocking reagents to inhibit endogenous peroxidase activity and avoid non-specific binding. The sections were incubated at 4°C overnight with a primary antibody against cytokeratin 19 (CK19) (ab52625, Abcam, Cambridge, UK at 1:1,000 dilution), glypican-3 (GPC3) (B0025R, BD Biosciences, San Jose, CA, USA at 1:200 dilution) and β-Catenin (610153, BD Biosciences at 1:200 dilution), followed by incubation with a horseradish-peroxidase (HRP)-conjugated secondary antibody at room temperature for 1 h. Signals were developed using the DAB+ substrate chromogen system (Dako) and counterstained with hematoxylin. For IHC analysis, positive staining of CK19 and GPC3 was defined as ≥5% of tumor cells showing cytoplasmic expression (for CK19) and membranous and/or cytoplasmic expression (for GPC3), respectively. Staining was estimated with reference to the percentage of tumor cells showing

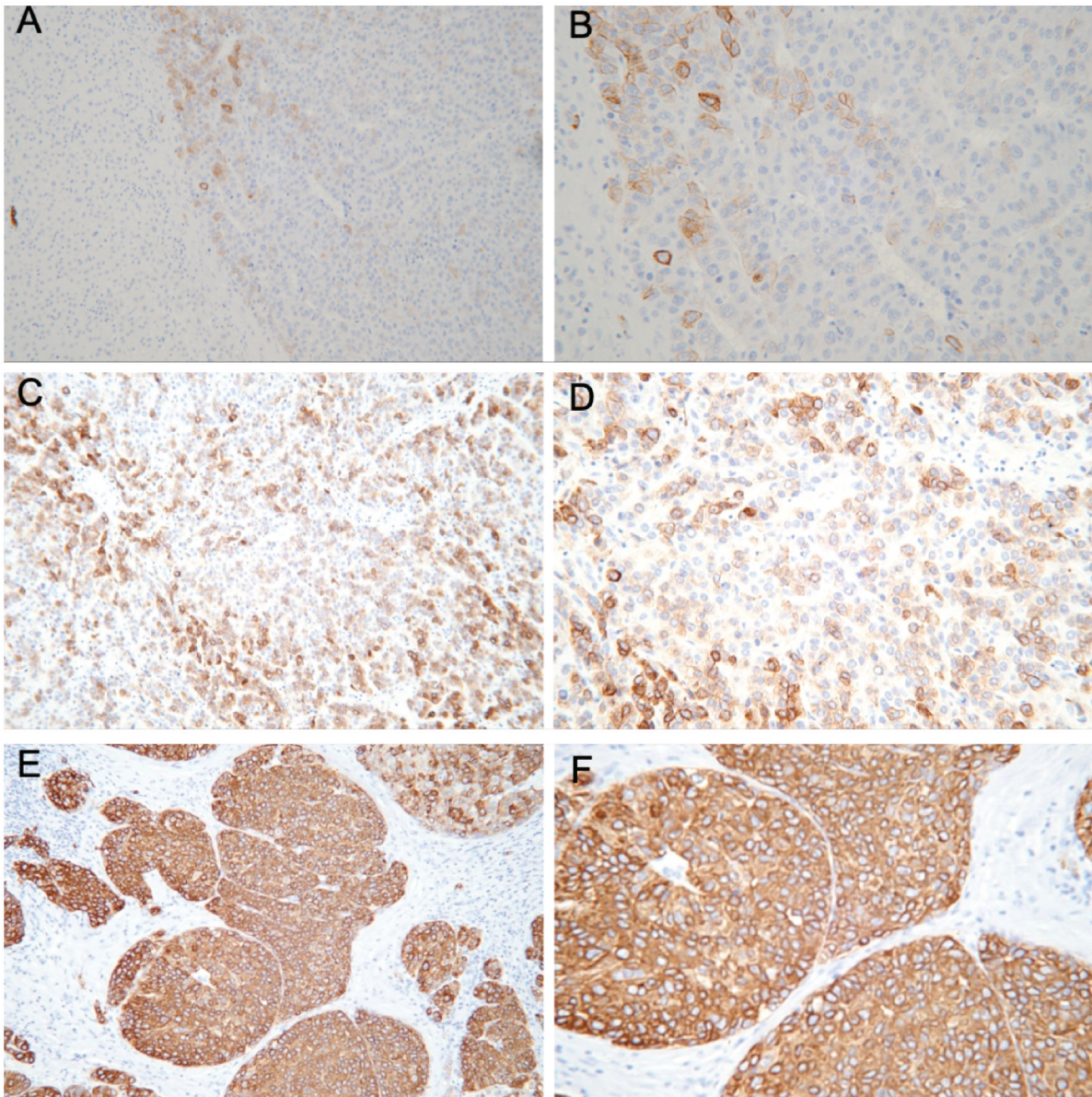


Figure 1. IHC expression of CK19 in HCC. Focal cytoplasmic pattern with weak staining intensity on 5% of tumor cells, (A) magnification $\times 100$, (B) magnification $\times 200$. Diffuse cytoplasmic pattern with moderate to strong staining intensity in 50% tumor cells, (C) magnification $\times 100$ (D) magnification $\times 200$. Diffuse cytoplasmic pattern with strong staining intensity in 90% of tumor cells, (E) magnification $\times 100$, (F) magnification $\times 200$.

positive staining. Cytoplasmic and/or nuclear accumulation of β -catenin was regarded as β -catenin overexpression. Staining was estimated with reference to the percentage of tumor cells showing positive staining, and scored to the nearest 5%.

Statistical analysis. Clinical data were retrieved from patients' records. Overall survival was defined as the interval from the date of surgery to death or last follow up. Recurrence-free survival was defined as the interval from the date of surgery to recurrence, death or last follow up. Kaplan–Meier curves were used to analyze survival. Correlation between CK19 and GPC3 expression was

analyzed using Fisher's exact test. Statistical significance was analyzed using Prism 8 software (GraphPad, San Diego, CA, USA) and defined as $p < 0.05$.

Results

Clinicopathological features of the cohort. Thirty-six cases were recruited to the study comprising 27 males and 9 females. The median age was 32 years, with a range between 9 and 40 years. Thirteen patients presented with multiple

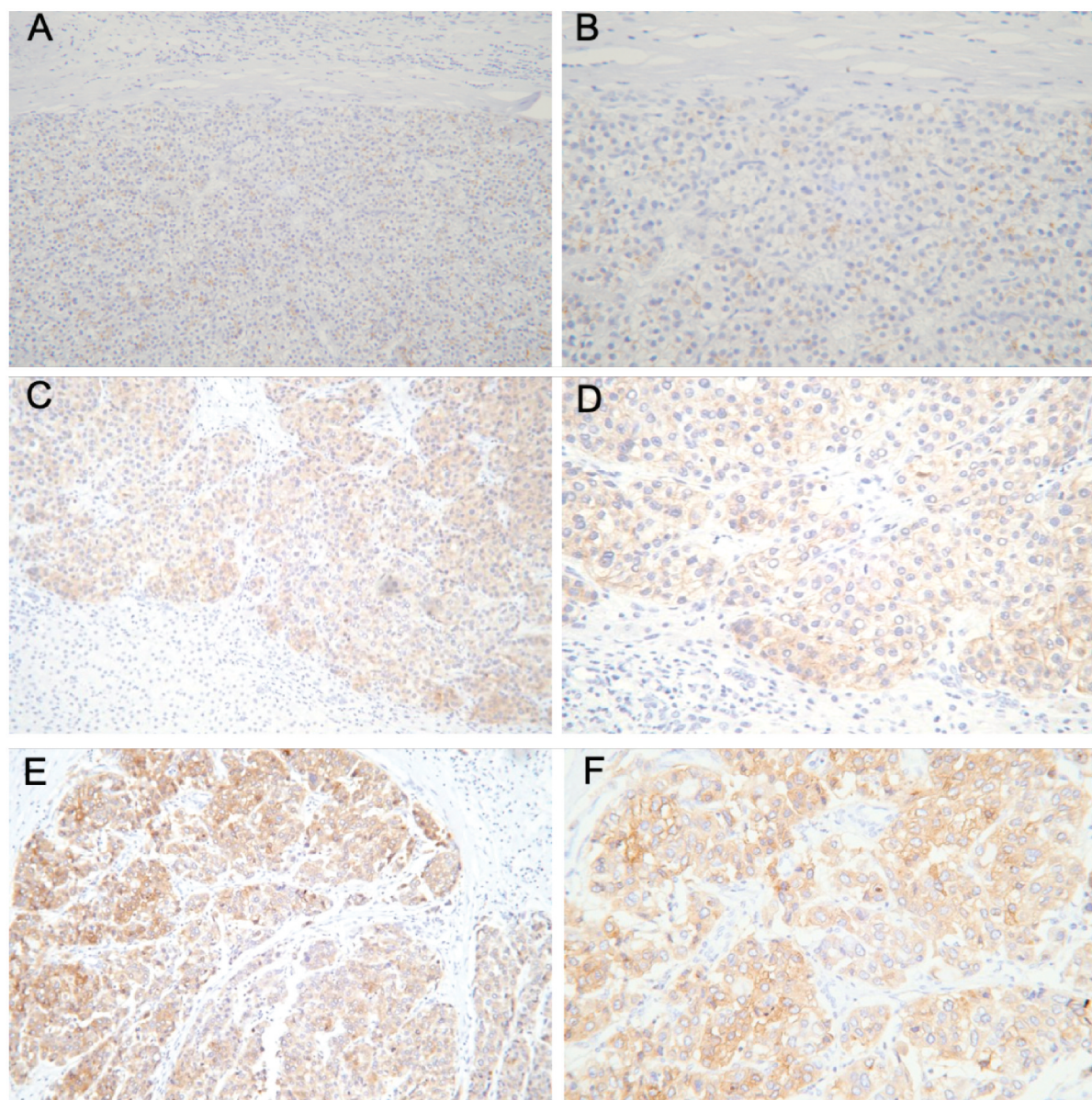


Figure 2. Immunohistochemical expression of GPC3 in HCC. Focal cytoplasmic pattern with weak staining intensity in 5% of tumor cells, (A) magnification $\times 100$, (B) magnification $\times 200$. Diffuse cytoplasmic pattern with moderate to strong staining intensity in 50% tumor cells, (C) magnification $\times 100$ (D) magnification $\times 200$. Diffuse cytoplasmic pattern with strong staining intensity in 90% of tumor cells, (E) magnification $\times 100$, (F) magnification $\times 200$.

nodules and the median size of the largest nodule was 9.5 cm. Single nodule was found in 23 patients and the median size was 3.8 cm. Twenty-nine patients (80.5%) suffered from HBV infection and two patients (5.5%) had HCV infection. Five patients (14%) were not known to have any predisposing primary liver diseases. The median preoperative serum AFP levels were 705.5 IU/ml (range=2-524,062.8 IU/ml). The clinicopathological parameters are summarized in Table II.

Table III. Correlation of CK19 and GPC3 expression assayed by immunohistochemistry.

| | GPC3+ | GPC3- | <i>p</i> -Value (Fisher's exact test) |
|-------|-------|-------|--|
| CK19+ | 16 | 6 | 0.016 |
| CK19- | 4 | 10 | |

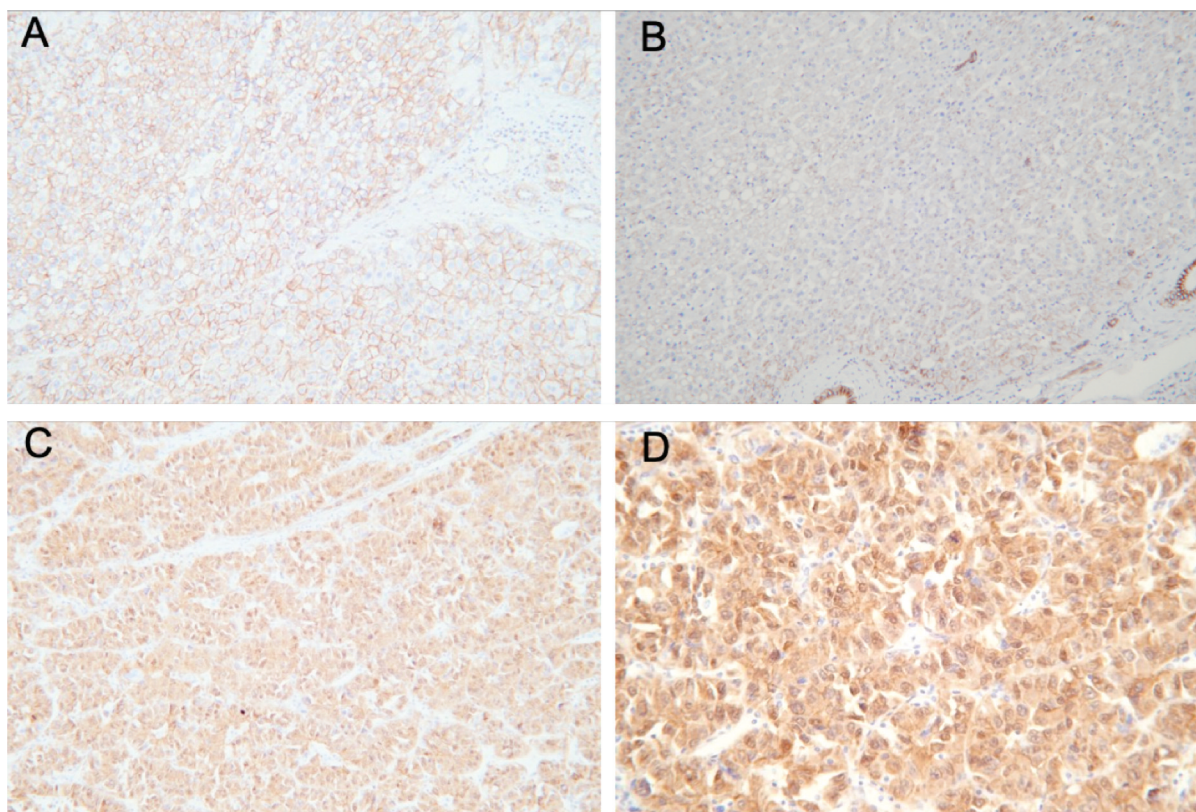


Figure 3. Immunohistochemical expression of β -catenin. Membranous pattern is observed in the (A) tumor region, and weak membranous pattern is observed in the (B) non-tumor region in a case showing no β -catenin overexpression. Magnification $\times 100$. Diffuse cytoplasmic and nuclear pattern with strong staining intensity is observed in a case positive for β -catenin over-expression, (C) magnification $\times 100$, (D) magnification $\times 200$.

Immunohistochemical expression of CK19, GPC3 and β -catenin in HCC. CK19 was expressed in 22 (61%) of 36 cases, while GPC3 was expressed in 20 (56%) cases (Figure 1). The majority of CK19+ (19/22) and GPC3+ HCC (15/20) was associated with 5-70% staining (Figure 2). Three CK19+ and 5 GPC3+ HCCs showed a strong and diffuse expression pattern (80-90%) with strong staining intensity. Comparing the IHC expression of CK19 and GPC3, the immunoreactivities of CK19 and GPC3 were positively correlated ($p=0.016$) (Table III). For β -catenin, membranous staining was present in tumor cells in all cases. Only one case (3%) demonstrated β -catenin over-expression with a strong cytoplasmic and nuclear staining intensity (Figure 3).

TP53 hotspot mutation analysis. Thirty-four cases were examined for TP53 mutations in exons 5 and 7, and two cases were excluded due to suboptimal DNA quality. Among the 34 cases, 4 demonstrated a hotspot TP53 mutation. One case (HCC-6) harbored V157F, while the R249S mutation in exon 7 was found in HCC-18, HCC-26, and HCC-30 (Figure 4). None of these cases harbored both V157F and R249S

mutations. All 4 mutated cases were associated with HBV infection. Preoperative AFP levels of HCC-6, HCC-18, HCC-26, and HCC-30 were 174,051 IU/ml, 631 IU/ml, 1,648 IU/ml and 524,063 IU/ml, respectively. One case was associated with a single tumor nodule; the other three cases had multiple nodules. Regarding the respective IHC results, all 4 cases were negative for β -catenin accumulation but demonstrated varying expression of CK19 and GPC3 (Table IV). At the time of writing, three patients died of disease; one patient defaulted follow up (HCC-26). Recurrence was observed in one case (HCC-18) with a recurrence-free survival of 124 days.

Correlation between clinicopathological parameters and survival outcome. The follow up period was 10 to 5,541 days (median: 805 days). Of these 36 patients, as of last follow up date, 16 patients died of the disease, 14 were alive with no evidence of disease, and 4 were alive with the disease. There were 2 defaulters. The median overall survival was 867 days (range=71-5,541 days). Recurrence was observed in 21 patients with a median recurrence-free survival of 178 days.

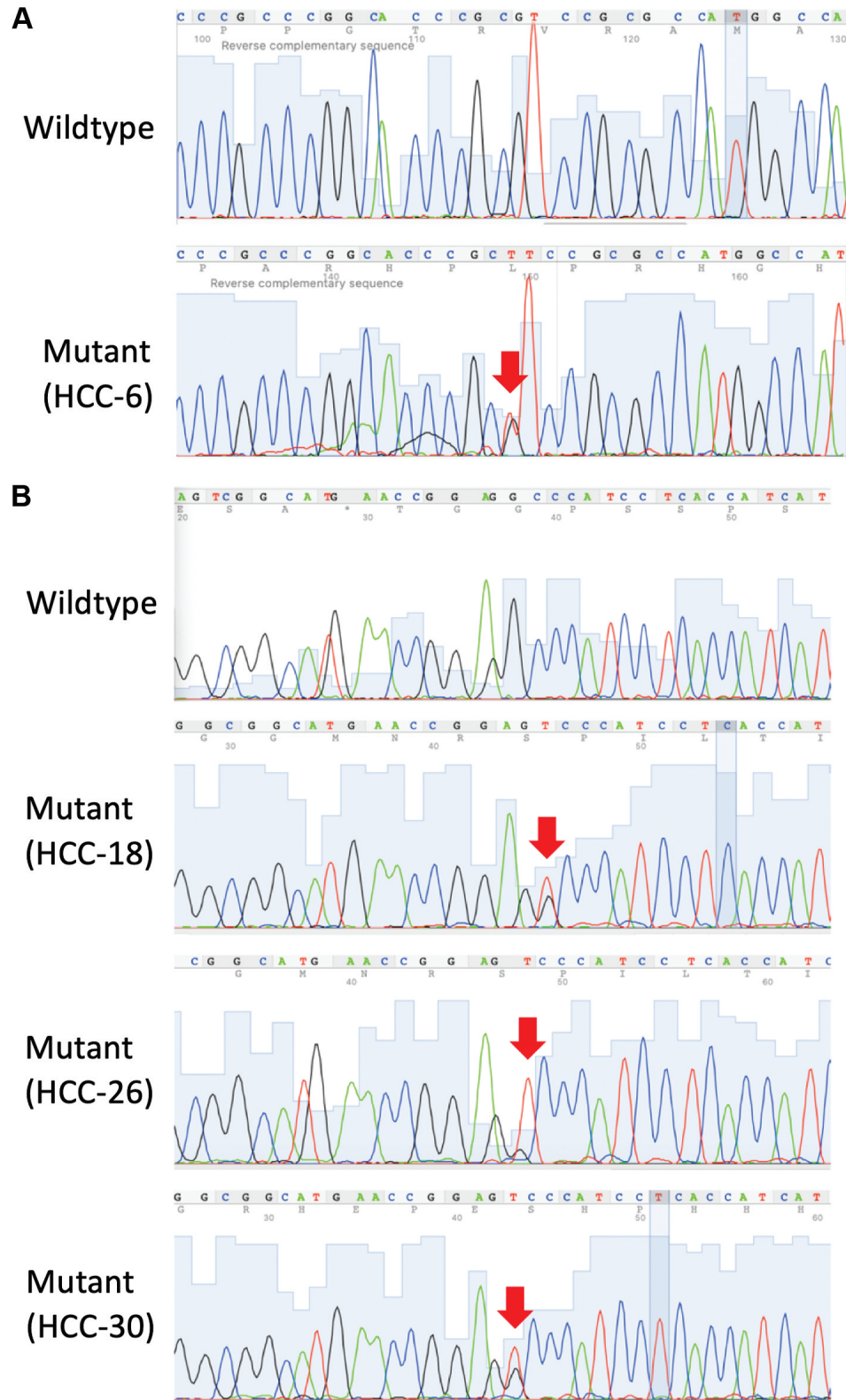


Figure 4. Sequencing analysis of TP53 exons 5 and 7. (A) Sequencing analysis of TP53 exon 5. Upper panel - Tumor tissue with wild type TP53 exon 5. Lower panel - Tumor tissue harboring V157F. (B) Sequencing analysis of TP53 exon 7. Upper panel - tumor tissue with wild type TP53 exon 7. Middle and lower panels - Tumor tissue harboring R249S. Arrows indicate the mutation sites.

Table IV. Immunohistochemical staining and TP53 mutation analysis results.

| Case ID | Immunohistochemistry | | | TP53 mutation | |
|---------|----------------------|-------|------------|---------------|--------|
| | CK19 | GPC-3 | β-catenin* | Exon 5 | Exon 7 |
| HCC-1 | 10 | 70 | – | WT | WT |
| HCC-2 | 0 | 0 | – | WT | WT |
| HCC-3 | 90 | 10 | – | WT | WT |
| HCC-4 | 70 | 30 | – | WT | WT |
| HCC-5 | 0 | 0 | – | WT | WT |
| HCC-6 | 0 | 0 | – | V157F | WT |
| HCC-7 | 20 | 5 | – | WT | WT |
| HCC-8 | 30 | 90 | – | WT | WT |
| HCC-9 | 90 | 10 | – | WT | WT |
| HCC-10 | 0 | 0 | – | WT | WT |
| HCC-11 | 50 | 90 | – | WT | WT |
| HCC-12 | 50 | 40 | – | WT | WT |
| HCC-13 | 20 | 50 | – | WT | WT |
| HCC-14 | 10 | 60 | – | WT | WT |
| HCC-15 | 20 | 5 | – | WT | WT |
| HCC-16 | 0 | 10 | – | WT | WT |
| HCC-17 | 0 | 90 | – | WT | WT |
| HCC-18 | 20 | 80 | – | WT | R249S |
| HCC-19 | 20 | 0 | – | WT | WT |
| HCC-20 | 0 | 0 | – | N/A | N/A |
| HCC-21 | 0 | 0 | – | WT | WT |
| HCC-22 | 20 | 0 | – | WT | WT |
| HCC-23 | 0 | 40 | – | WT | WT |
| HCC-24 | 0 | 60 | – | WT | WT |
| HCC-25 | 10 | 0 | – | N/A | N/A |
| HCC-26 | 30 | 30 | – | WT | R249S |
| HCC-27 | 0 | 0 | – | WT | WT |
| HCC-28 | 0 | 0 | – | WT | WT |
| HCC-29 | 50 | 70 | – | WT | WT |
| HCC-30 | 30 | 0 | – | WT | R249S |
| HCC-31 | 50 | 0 | – | WT | WT |
| HCC-32 | 0 | 0 | – | WT | WT |
| HCC-33 | 0 | 0 | – | WT | WT |
| HCC-34 | 30 | 90 | – | WT | WT |
| HCC-35 | 80 | 5 | + | WT | WT |
| HCC-36 | 70 | 0 | – | WT | WT |

*Nuclear accumulation of β-catenin; WT: wild type; N/A: no sequencing results available.

A significant correlation between overall survival and number of tumor nodules ($p=0.011$), vascular invasion ($p=0.0074$), and preoperative AFP levels ($p=0.011$), was found (Figure 5A-C). The recurrence-free survival was correlated with the number of tumor nodules ($p=0.015$) and vascular invasion ($p=0.014$) (Figure 5D and E). The IHC expression was then correlated with the survival outcome. The median overall survival of CK19+ and CK19– groups were 867 and 939 days ($p=0.61$), respectively. For GPC3, the median overall survival of the GPC3+ and GPC3– groups was 936 and 765.5 days ($p=0.72$), respectively. The median recurrence-free survival of the CK19+ and CK19– groups was 399.5 and 468 days

($p=0.88$), respectively. For GPC3, the median recurrence-free survival time of the GPC3+ and GPC3– groups was 446 and 410.5 days ($p=0.74$), respectively. No significant correlation between CK19 or GPC3 and overall survival or recurrence-free survival was observed (Figure 6A and B). CK19 and GPC3 were co-expressed (CK19+/GPC3+) in 14 cases; 10 cases showed no CK19 or GPC3 expression (CK19–/GPC3–). There was no significant difference in overall survival between CK19+/GPC3+ and CK19–/GPC3– groups ($p=0.84$) (Figure 6C).

Discussion

In the current study, we reported the clinicopathological features and expression of some well-characterized biomarkers in a cohort of young-onset HCC. Similar to the general HCC population, young-onset HCC showed male predominance with a ratio of 3:1 and the majority of HCCs associated with HBV infection. Consistent with reported studies on HCC cohorts, young-onset HCC commonly expressed GPC3. On the other hand, the expression of CK19 was notably higher (61%) in our young-onset HCC cohort compared to results from other studies (10-30%). Klein *et al.* demonstrated the immunoreactivity of CK19 in HCC patients under 30 years of age, in which 22% (2/9) of cases were CK19 positive (29). The enhanced CK19 expression in our cohort possibly indicates an increased stemness signature of HCC in this subset of patients. Of note, young-onset HCC resulted in similar postoperative recurrence rate but presented a robust reduction in time to recurrence. The median time to recurrence ranges from 12.5 to 23 months based on previous reports (11, 30). In the present study, 72.4% of HCC patients experienced recurrence, with a median recurrence-free survival of only 5.9 months (178 days).

Previous reports have also indicated that expression of CK19 and GPC3 exhibits an adverse effect on HCC prognosis. In a study by Feng *et al.* (11), co-expression of CK19 and GPC3 was found to be associated with more aggressive disease and a higher risk of intrahepatic or extrahepatic metastasis, microvascular invasion, and regional lymph node involvement, when compared to CK19–/GPC3+ and CK19–/GPC3– HCC. In the same study, median recurrence-free survival of CK19+/GPC3+ HCC patients was shorter than that of CK19–/GPC3– groups (10 vs. 43 months). In contrast, despite the positive correlation between CK19 and GPC expression, no significant difference in survival was observed in our cohort (CK19+ vs. CK19–, $p=0.61$; GPC3+ vs. GPC3–, $p=0.72$). Regarding TP53 mutation, our young-onset HCC cases demonstrated a lower mutation rate in both R249S and V157F. Besides, in the present study, only 1 case (4.5%) showed β-catenin accumulation, suggesting a lower activation rate of β-catenin pathway in young-onset HCC. However, considering the cohort size, further studies are required. In our young-onset

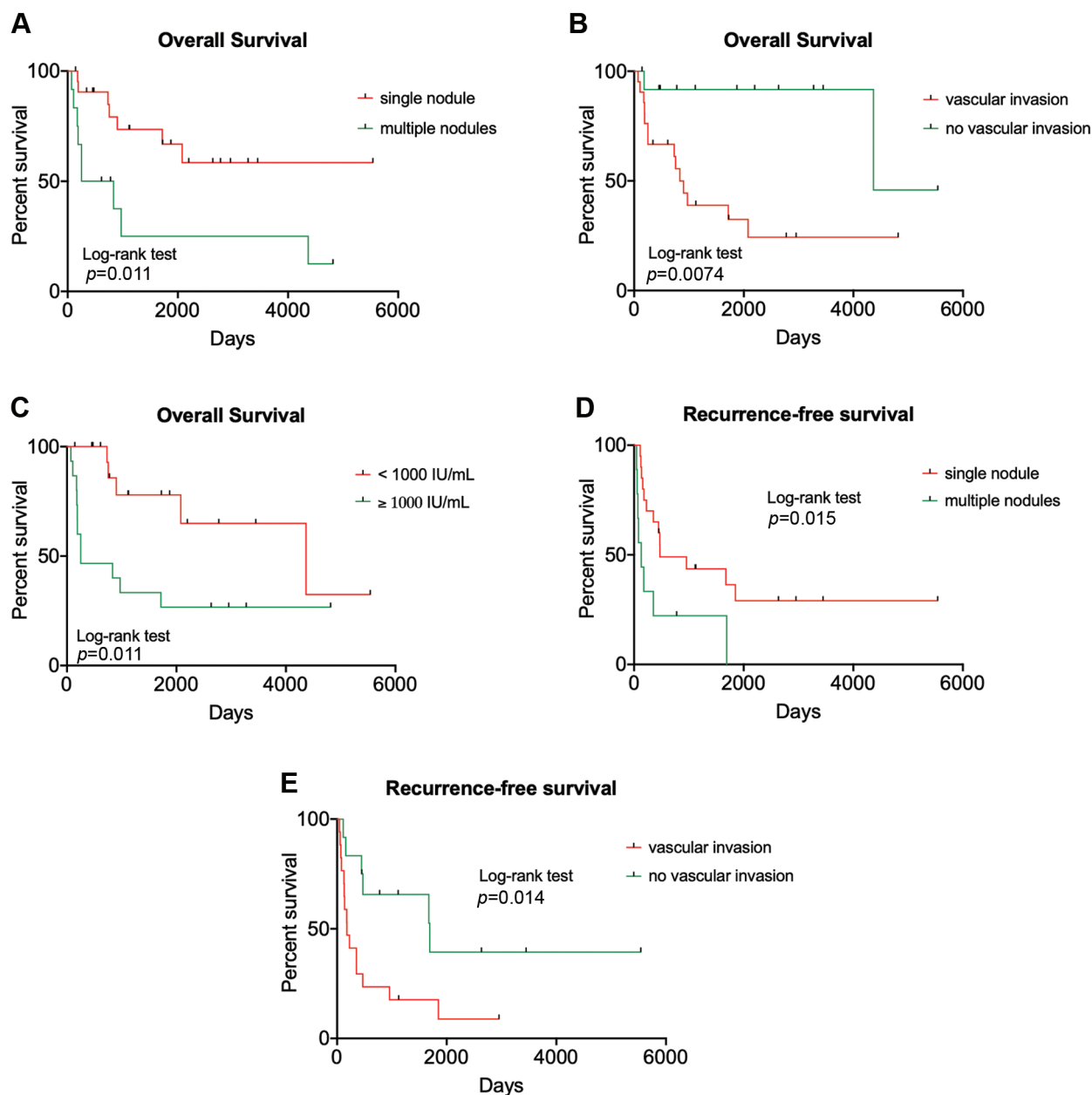


Figure 5. Kaplan-Meier curves for overall survival with reference to (A) number of tumor nodules; (B) vascular invasion, and (C) preoperative AFP levels. Kaplan-Meier curves for recurrence-free survival with reference to (D) number of tumor nodules and (E) vascular invasion.

HCC cases, vascular invasion, preoperative AFP levels and the number of tumor nodules were correlated with survival.

Our study has some limitations. The use of FFPE tissues could have introduced DNA fragmentation thus, restricting the primer design process. To optimize the target sequence length for each set of primers, three different housekeeping genes with target product length of around 100 bp, 200 bp and 300 bp were used to estimate the approximate size of the

DNA fragment of the sample. In this study, primers were designed for a target product within 150 bp. Second, expansion of the cohort size could have possibly facilitated more definitive results from the statistical analyses.

Conflicts of Interest

All Authors declare no conflicts of interest in relation to this study.

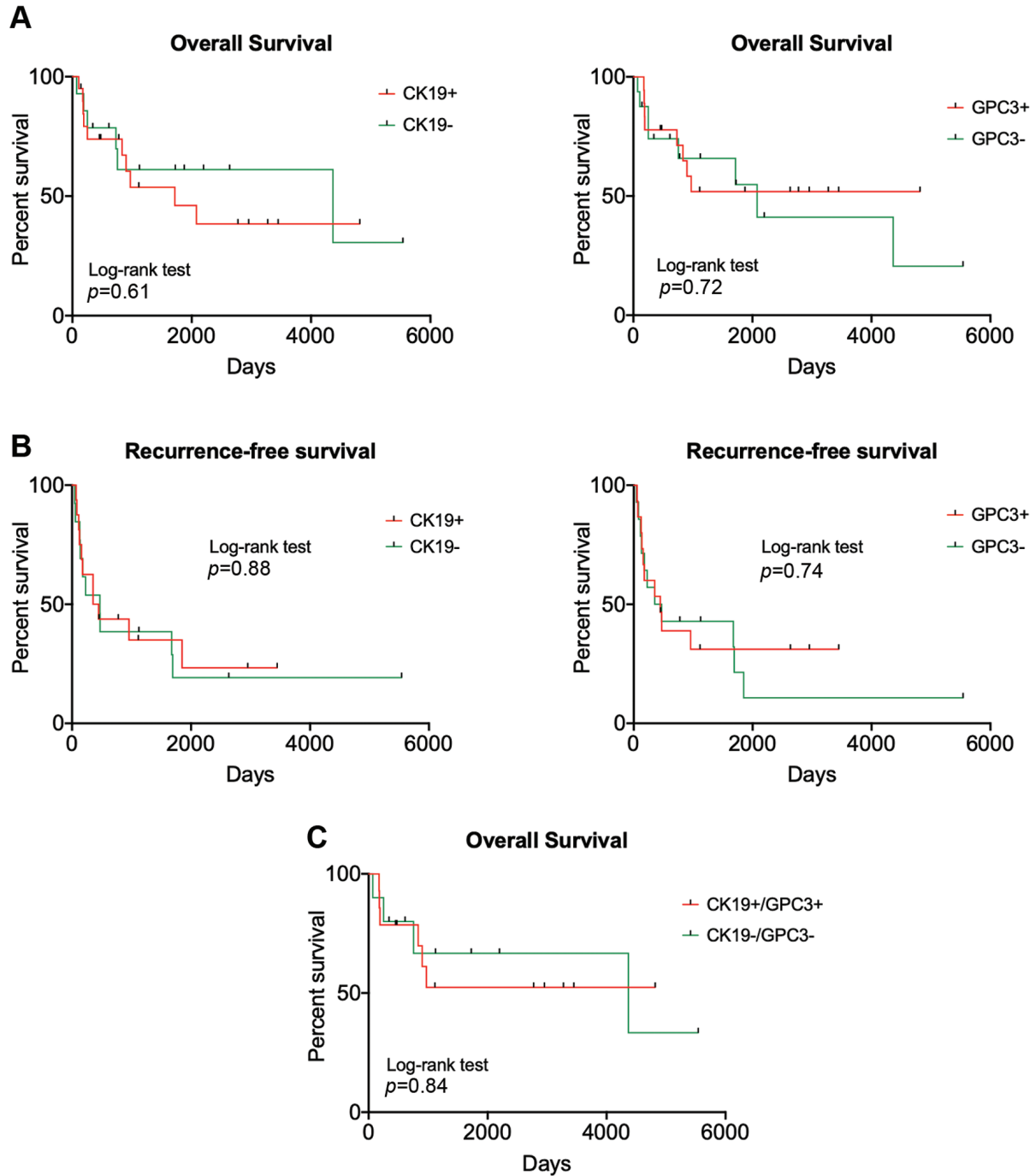


Figure 6. Kaplan–Meier curves for (A) overall survival and (B) recurrence-free survival in (left panel) CK19+ versus CK19- groups and (right panel) GPC3+ versus GPC3- groups. (C) Kaplan–Meier curves for overall survival in CK19+/GPC3+ versus CK19-/GPC3- groups.

Authors' Contributions

Study conception and design: R.C.L.; Data acquisition: K.A., K.K.C.; Data analysis: K.A., K.K.C., R.C.L.; Writing of manuscript: K.A., R.C.L.

Acknowledgements

The Authors thank Mr Eddie Lo, Department of Pathology, Queen Mary Hospital, Hong Kong, P.R. China for the technical support.

References

- Emre S and McKenna GJ: Liver tumors in children. *Pediatr Transplant* 8(6): 632-638, 2004. PMID: 15598339. DOI: 10.1111/j.1399-3046.2004.00268.x
- Yang JD, Hainaut P, Gores GJ, Amadou A, Plymoth A and Roberts LR: A global view of hepatocellular carcinoma: trends, risk, prevention and management. *Nat Rev Gastroenterol Hepatol* 16(10): 589-604, 2019. PMID: 31439937. DOI: 10.1038/s41575-019-0186-y
- Cowell E, Patel K, Heczey A, Finegold M, Venkatramani R, Wu H, López-Terrada D and Miloh T: Predisposing conditions to pediatric hepatocellular carcinoma and association with outcomes: single-center experience. *J Pediatr Gastroenterol Nutr* 68(5): 695-699, 2019. PMID: 30676520. DOI: 10.1097/MPG.0000000000002285
- Khanna R and Verma SK: Pediatric hepatocellular carcinoma. *World J Gastroenterol* 24(35): 3980-3999, 2018. PMID: 30254403. DOI: 10.3748/wjg.v24.i35.3980
- Lau CS, Mahendraraj K and Chamberlain RS: Hepatocellular carcinoma in the pediatric population: a population based clinical outcomes study involving 257 patients from the surveillance, epidemiology, and end result (SEER) database (1973-2011). *HPB Surg* 2015: 670728, 2015. PMID: 26663981. DOI: 10.1155/2015/670728
- Ho DW, Lo RC, Chan LK and Ng IO: Molecular pathogenesis of hepatocellular carcinoma. *Liver Cancer* 5(4): 290-302, 2016. PMID: 27781201. DOI: 10.1159/000449340
- Haines K, Sarabia SF, Alvarez KR, Tomlinson G, Vasudevan SA, Heczey AA, Roy A, Finegold MJ, Parsons DW, Plon SE and López-Terrada D: Characterization of pediatric hepatocellular carcinoma reveals genomic heterogeneity and diverse signaling pathway activation. *Pediatr Blood Cancer* 66(7): e27745, 2019. PMID: 30977242. DOI: 10.1002/psc.27745
- Kan Z, Zheng H, Liu X, Li S, Barber TD, Gong Z, Gao H, Hao K, Willard MD, Xu J, Hauptschein R, Rejto PA, Fernandez J, Wang G, Zhang Q, Wang B, Chen R, Wang J, Lee NP, Zhou W, Lin Z, Peng Z, Yi K, Chen S, Li L, Fan X, Yang J, Ye R, Ju J, Wang K, Estrella H, Deng S, Wei P, Qiu M, Wulur IH, Liu J, Ehsani ME, Zhang C, Loboda A, Sung WK, Aggarwal A, Poon RT, Fan ST, Wang J, Hardwick J, Reinhard C, Dai H, Li Y, Luk JM and Mao M: Whole-genome sequencing identifies recurrent mutations in hepatocellular carcinoma. *Genome Res* 23(9): 1422-1433, 2013. PMID: 23788652. DOI: 10.1101/gr.154492.113
- Yuan RH, Jeng YM, Hu RH, Lai PL, Lee PH, Cheng CC and Hsu HC: Role of p53 and β -catenin mutations in conjunction with CK19 expression on early tumor recurrence and prognosis of hepatocellular carcinoma. *J Gastrointest Surg* 15(2): 321-329, 2011. PMID: 21061181. DOI: 10.1007/s11605-010-1373-x
- Kim H, Choi GH, Na DC, Ahn EY, Kim GI, Lee JE, Cho JY, Yoo JE, Choi JS and Park YN: Human hepatocellular carcinomas with "Stemness"-related marker expression: keratin 19 expression and a poor prognosis. *Hepatology* 54(5): 1707-1717, 2011. PMID: 22045674. DOI: 10.1002/hep.24559
- Feng J, Zhu R, Chang C, Yu L, Cao F, Zhu G, Chen F, Xia H, Lv F, Zhang S and Sun L: CK19 and Glypican 3 Expression Profiling in the Prognostic Indication for Patients with HCC after Surgical Resection. *PLoS One* 11(3): e0151501, 2016. PMID: 26977595. DOI: 10.1371/journal.pone.0151501
- Lee JI, Lee JW, Kim JM, Kim JK, Chung HJ and Kim YS: Prognosis of hepatocellular carcinoma expressing cytokeratin 19: comparison with other liver cancers. *World J Gastroenterol* 18(34): 4751-4757, 2012. PMID: 23002345. DOI: 10.3748/wjg.v18.i34.4751
- Lo RC and Ng IO: Hepatocellular tumors: immunohistochemical analyses for classification and prognostication. *Chin J Cancer Res* 23(4): 245-253, 2011. PMID: 23359751. DOI: 10.1007/s11670-011-0245-6
- Wang HL, Anatelli F, Zhai QJ, Adley B, Chuang ST and Yang XJ: Glypican-3 as a useful diagnostic marker that distinguishes hepatocellular carcinoma from benign hepatocellular mass lesions. *Arch Pathol Lab Med* 132(11): 1723-1728, 2008. PMID: 18976006. DOI: 10.1043/1543-2165-132.11.1723
- Xiao WK, Qi CY, Chen D, Li SQ, Fu SJ, Peng BG and Liang LJ: Prognostic significance of glypican-3 in hepatocellular carcinoma: a meta-analysis. *BMC Cancer* 14: 104, 2014. PMID: 24548704. DOI: 10.1186/1471-2407-14-104
- Harding JJ, Nandakumar S, Armenia J, Khalil DN, Albano M, Ly M, Shia J, Hechtman JF, Kundra R, El Dika I, Do RK, Sun Y, Kingham TP, D'Angelica MI, Berger MF, Hyman DM, Jarnagin W, Klimstra DS, Janjigian YY, Solit DB, Schultz N and Abou-Alfa GK: Prospective genotyping of hepatocellular carcinoma: Clinical implications of next-generation sequencing for matching patients to targeted and immune therapies. *Clin Cancer Res* 25(7): 2116-2126, 2019. PMID: 30373752. DOI: 10.1158/1078-0432.CCR-18-2293
- Huang FY, Wong DK, Tsui VW, Seto WK, Mak LY, Cheung TT, Lai KK and Yuen MF: Targeted genomic profiling identifies frequent deleterious mutations in FAT4 and TP53 genes in HBV-associated hepatocellular carcinoma. *BMC Cancer* 19(1): 789, 2019. PMID: 31395065. DOI: 10.1186/s12885-019-6002-9
- Woo HG, Wang XW, Budhu A, Kim YH, Kwon SM, Tang ZY, Sun Z, Harris CC and Thorgeirsson SS: Association of TP53 mutations with stem cell-like gene expression and survival of patients with hepatocellular carcinoma. *Gastroenterology* 140(3): 1063-1070, 2011. PMID: 21094160. DOI: 10.1053/j.gastro.2010.11.034
- Villanueva A and Hoshida Y: Depicting the role of TP53 in hepatocellular carcinoma progression. *J Hepatol* 55(3): 724-725, 2011. PMID: 21616106. DOI: 10.1016/j.jhep.2011.03.018
- Okabe H, Kinoshita H, Imai K, Nakagawa S, Higashi T, Arima K, Uchiyama H, Ikegami T, Harimoto N, Itoh S, Ishiko T, Yoshizumi T, Beppu T, Monga SP, Baba H and Maehara Y: Diverse basis of β -catenin activation in human hepatocellular carcinoma: implications in biology and prognosis. *PLoS One* 11(4): e0152695, 2016. PMID: 27100093. DOI: 10.1371/journal.pone.0152695
- Calderaro J, Couchy G, Imbeaud S, Amadeo G, Letouze E, Blanc JF, Laurent C, Hajji Y, Azoulay D, Bioulac-Sage P, Nault JC and Zucman-Rossi J: Histological subtypes of hepatocellular carcinoma are related to gene mutations and molecular tumour classification. *J Hepatol* 67(4): 727-738, 2017. PMID: 28532995. DOI: 10.1016/j.jhep.2017.05.014
- Zhan P, Ji YN and Yu LK: TP53 mutation is associated with a poor outcome for patients with hepatocellular carcinoma: evidence from a meta-analysis. *Hepatobiliary Surg Nutr* 2(5): 260-265, 2013. PMID: 24570956. DOI: 10.3978/j.issn.2304-3881.2013.07.06
- Khalaf AM, Fuentes D, Morshid AI, Burke MR, Kaseb AO, Hassan M, Hazle JD and Elsayes KM: Role of Wnt/ β -catenin signaling in hepatocellular carcinoma, pathogenesis, and clinical significance. *J Hepatocell Carcinoma* 5: 61-73, 2018. PMID: 29984212. DOI: 10.2147/JHC.S156701

- 24 Tornesello ML, Buonaguro L, Tatangelo F, Botti G, Izzo F and Buonaguro FM: Mutations in TP53, CTNNB1 and PIK3CA genes in hepatocellular carcinoma associated with hepatitis B and hepatitis C virus infections. *Genomics* 102(2): 74-83, 2013. PMID: 23583669. DOI: 10.1016/j.ygeno.2013.04.001
- 25 Vilchez V, Turcios L, Marti F and Gedaly R: Targeting Wnt/ β -catenin pathway in hepatocellular carcinoma treatment. *World J Gastroenterol* 22(2): 823-832, 2016. PMID: 26811628. DOI: 10.3748/wjg.v22.i2.823
- 26 Kondo Y, Kanai Y, Sakamoto M, Genda T, Mizokami M, Ueda R and Hirohashi S: Beta-catenin accumulation and mutation of exon 3 of the beta-catenin gene in hepatocellular carcinoma. *Jpn J Cancer Res* 90(12): 1301-1309, 1999. PMID: 10665646. DOI: 10.1111/j.1349-7006.1999.tb00712.x
- 27 Nhieu JT, Renard CA, Wei Y, Cherqui D, Zafrani ES and Buendia MA: Nuclear accumulation of mutated beta-catenin in hepatocellular carcinoma is associated with increased cell proliferation. *Am J Pathol* 155(3): 703-710, 1999. PMID: 10487827. DOI: 10.1016/s0002-9440(10)65168-1
- 28 Wong CM, Fan ST and Ng IO: beta-Catenin mutation and overexpression in hepatocellular carcinoma: clinicopathologic and prognostic significance. *Cancer* 92(1): 136-145, 2001. PMID: 11443619. DOI: 10.1002/1097-0142(20010701)92:1<136::aid-cnrcr1301>3.0.co;2-r
- 29 Klein WM, Molmenti EP, Colombani PM, Grover DS, Schwarz KB, Boitnott J and Torbenson MS: Primary liver carcinoma arising in people younger than 30 years. *Am J Clin Pathol* 124(4): 512-518, 2005. PMID: 16146811. DOI: 10.1309/TT0R7KAL32228E99
- 30 Bürger C, Maschmeier M, Hüsing-Kabar A, Wilms C, Köhler M, Schmidt M, Schmidt HH and Kabar I: Achieving complete remission of hepatocellular carcinoma: a significant predictor for recurrence-free survival after liver transplantation. *Can J Gastroenterol Hepatol* 2019: 5796074, 2019. PMID: 30729099. DOI: 10.1155/2019/5796074

Received April 22, 2021

Revised May 12, 2021

Accepted May 13, 2021